Photouncaging of ceramides promotes reorganization of liquid-ordered domains in supported lipid bilayers

Carter Ramirez, Daniel M.; Pitre, Spencer P.; Kim, Young Ah; Bittman, Robert; Johnston, Linda J.

Publisher's version / Version de l'éditeur:
https://doi.org/10.1021/la3039158
Langmuir, 29, 10, pp. 3380-3387, 2013-02-12

Photo-uncaging of Short and Long-Chain Ceramides Promotes Reorganization of Liquid-Ordered Domains in Supported Lipid Bilayers

Daniel M. Carter Ramirez,[†,$] Spencer P. Pitre,[†] Young Ah Kim,[#] Robert Bittman,[#] and Linda J. Johnston[†]

[†] *National Research Council of Canada, Ottawa, ON K1A 0R6, CANADA*

[$] *Department of Chemistry, University of Ottawa, Ottawa, ON K1N 6N5, CANADA*

[#] *Department of Chemistry and Biochemistry, Queens College of The City University of New York, Flushing, NY 11367, USA*

ABSTRACT: 6-bromo-7-hydroxycoumarin caged ceramides were incorporated in supported lipid bilayers with a mixture of coexisting liquid-ordered (L_o) and liquid-disordered (L_d) phases. Release of C4 and C16 Cer by photolysis using long wavelength UV light was studied using a combination of atomic force and fluorescence microscopies, demonstrating the ability to generate Cer with spatial and temporal control. The generation of C16-Cer disrupts the L_o domains, resulting in the incorporation of small areas of fluid phase and the disappearance of some domains. Cer-rich gel-phase domains are not observed, by contrast to results obtained by either the direct incorporation of Cer or enzymatic Cer generation. These differences are hypothesized to reflect low incorporation of caged Cer in supported bilayers due to a heterogeneous population of vesicles and selective adsorption and rupture of vesicles containing low concentrations of caged Cer during bilayer formation. Photorelease of a short-chain Cer results in qualitatively similar results, with disappearance of some L_o domains, but also with a smaller height difference between the ordered and disordered phases. These results are consistent with literature results demonstrating that a short-chain Cer disrupts L_o domains and does not form Cer-rich gel phases, but may form mixed or partially interdigitated phases.

INTRODUCTION

Ceramide (Cer) is a raft-associated sphingolipid that has been implicated in diverse cellular processes, including differentiation, senescence, apoptosis and immune response.[1-4] Although Cer is present in relatively small amounts in resting cells, its concentration can reach levels of up to 10 mol% of the total lipid content in apoptotic cells.[3] It is produced by de novo synthesis, enzymatic hydrolysis of the phosphorylcholine head group of sphingomyelin (SM) and several other enzymatic routes. Cer is one of the most hydrophobic natural lipids and has significant effects on the biophysical properties of membranes, including its propensity to promote phase separation and the formation of gel-phase domains and to induce negative membrane curvature and either membrane permeabilization or membrane fusion.[5-8] Enzymatic generation of Cer in cells has also been shown to induce coalescence of small raft domains into larger signaling platforms, providing a mechanism for amplifying signaling by membrane receptors.[1, 2] Membrane rafts are small transient domains that are enriched in SM, cholesterol (Chol), and certain proteins; they are thought to exist in a liquid-ordered (L_o) phase that is distinct from the surrounding liquid-disordered (L_d) membrane and to play an important role in signal transduction.[9-12]

A number of studies have examined the effects of direct incorporation of Cer in supported bilayers that exhibit L_d/L_o phase separation, demonstrating the formation of a third Cer-enriched gel phase for some lipid mixtures.[13-16] Generation of Cer by sphingomyelinase (SMase) in similar phase-separated model membranes leads to extensive membrane restructuring that is considerably more complex to interpret than the results obtained by direct Cer incorporation.[14, 17-24] Using atomic force microscopy (AFM) combined with fluorescence, our previous work has identified a range of structural changes in SMase-treated supported lipid bilayers.[18, 21, 22, 25] These include the formation of Cer-rich regions in the original L_o domains, in addition to the complete disappearance of some domains with the concomitant formation of highly ordered dye-excluding and Chol-depleted membrane regions. The heterogeneity of model membranes containing SMase-generated Cer reflects the inherent difficulties in targeting and controlling the extent of enzyme activity in vitro.[17, 19, 22] Recently, the enzymatic generation of Cer in bilayers prepared in microfluidic channels has been investigated in an attempt to address these issues.[19] However, so far approaches using enzymatic Cer generation in model membranes have failed to reproduce the precise regulation of SMase activity and localized hydrolysis of SM that occur in cells. Thus, an approach for producing a known, controlled concentration of Cer within localized regions of bilayer membranes would be a significant advantage, both for model membranes and for probing biological pathways that are modulated by Cer.

Photolabile groups have been widely used to release bioactive molecules with both spatial and temporal control.[26-28] The covalent attachment of a photoremovable protecting group (cage) to the biomolecule of interest renders it biologically inactive until photolysis releases the active form and triggers specific biological activity. Although photodeprotection has been widely applied to release small molecule neurotransmitters and to study peptide and protein

function, there are only a few examples of photocaged lipids, notably for sphingosine 1-phosphate, ceramide-1-phosphate, ceramide and phosphatidylinositol-3,4,5-triphosphate.[29-32] In each case, the caged lipid is designed to be membrane permeable for delivery to cells and to release a lipid second messenger involved in a specific biological pathway. Several studies have also shown that various photoswitchable lipids can modulate the shape and phase separation behavior of vesicle bilayer membranes.[33-35]

We have recently reported the development of a photocaged dihydro-Cer that can be delivered into and released in cells.[29] Herein we describe the incorporation of similarly caged *N*-palmitoyl-D-*erythro*-sphingosine (C16-Cer, **1**) and *N*-butanoyl-D-*erythro*-sphingosine (C4-Cer, **2**) into phase-separated supported bilayers, which generate the corresponding Cers on photolysis with long wavelength UV light with a high degree of spatial and temporal control. Using correlated fluorescence-AFM, we have examined the structural reorganization that occurs when controlled quantities of C4- or C16-Cer are produced in bilayers with coexisting L_o and L_d phases. Despite the documented differences in biological activity between long- and short-chain ceramides, the two caged ceramides show similar effects on membrane morphology for the ternary lipid mixture examined herein.

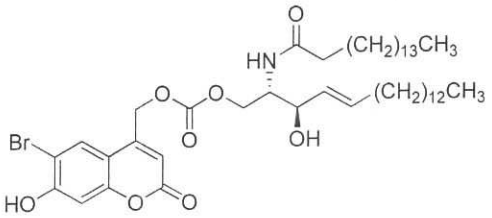

1

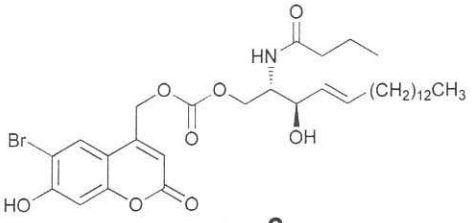

2

MATERIALS AND METHODS

Chemicals. 1,2-Dioleoyl-*sn*-glycero-3-phosphocholine (dioleoylphosphocholine, DOPC), egg sphingomyelin (ESM), *N*-palmitoyl-*D*-*erythro*-sphingosine (C16:0 ceramide, C16-Cer), and cholesterol were purchased from Avanti Polar Lipids (Alabaster, AL) and used without further purification. 1,1'-Dieicosanyl-3,3,3',3'-tetramethylindocarbocyanine perchlorate (DiI-C_{20}) was purchased from Molecular Targeting Technologies (Westchester, PA). (2*S*,3*R*,4*E*)-2-Palmitoylamido-3-hydroxyoctadec-4-enyl (6-bromo-7-hydroxycoumarin-4-yl)methyl carbonate (caged C16-Cer, **1**) and (2*S*,3*R*,4*E*)-2-butyramido-3-hydroxyoctadec-4-enyl (6-bromo-7-hydroxycoumarin-4-yl)methyl carbonate (caged C4-Cer, **2**) were synthesized as described previously and purified by preparative HPLC prior to use, where necessary. Optical adhesive 88 was obtained from Norland Products (Cranbury, NJ) and used to glue mica onto cover glass (Fisher Scientific, Hampton, NH). All aqueous solutions were prepared using 18.3 MΩ cm *Milli-Q* water. KMops buffer (100 mM KCl, 10 mM 3-(*N*-morpholino)-propanesulfonate (Mops), pH 7.4) was used for some imaging and photolysis experiments. Buffered solutions were passed through a 0.22 μm filter (Millipore, Billerica, MA) before use.

Supported lipid bilayers. Small unilamellar vesicles (SUVs) were prepared as previously described subject to some minor modifications.[25] Lipids, caged Cer, and DiI-C_{20} were dissolved in chloroform, methanol, ethanol, or mixtures thereof as required. After these solutions were mixed in appropriate amounts, the solvents were evaporated and the dry lipid films were hydrated in *Milli-Q* water and sonicated at 60 °C in a bath sonicator to clarity to form SUVs with a final lipid concentration of 0.5 mg/mL. Lipid films were stored for up to 1 week at -20 °C prior to use; however, fresh vesicles were prepared for each imaging experiment.

Planar supported bilayers were formed on mica via vesicle fusion. Freshly cleaved mica disks (15-25 μm thick for fluorescence imaging) were glued onto circular cover glasses. To prepare bilayers of DOPC/ESM/Chol/caged Cer, 950 μL of 8 mM $CaCl_2$ was first added to a mica/glass slide clamped in a liquid cell, and warmed to 45 °C. Aliquots (20-50 μL) of vesicle suspension were introduced at the same temperature, and the samples were incubated for 15 min before being gradually cooled to 22 °C over a period of 2 h. Bilayers were gently washed with *Milli-Q* water or KMops buffer to remove unattached vesicles before imaging.

Fluorescence microscopy and correlated fluorescence-atomic force microscopy. Fluorescence imaging and correlated fluorescence-atomic force microscopy were performed on the same microscope platform at room temperature (~22 °C). The imaging system consisted of a NanoWizard II BioAFM (JPK Instruments, Berlin, Germany) integrated with an IX81 inverted optical microscope (Olympus Corporation, Tokyo, Japan). Epifluorescence images were obtained using lamp excitation with an Olympus UPlanSAPO 100x, NA = 1.4 oil immersion objective, Cy3 and DAPI filter sets (Chroma Technology, Bellows Falls, VT), and a high resolution CoolSNAP CCD camera (Semrock, AZ). Fluorescence images were scaled, cropped, and correlated with the corresponding AFM scans using Image J freeware (NIH, Bethesda, MD).

Caged Cer photolysis experiments were carried out on the same setup using the lamp and DAPI filter set. The aperture built into the microscope illuminator was used to confine UV irradiation of the sample to a hexagonal area ~25 μm in diameter. To assess uncaging ability, we irradiated an aqueous dispersion of **1** for several minutes on the fluorescence microscope. Post-UV HPLC analysis of the solution confirmed that photolysis of the caged lipid had taken place to afford C16-Cer and 6-bromo-7-hydroxycoumarin (data not shown).

AFM images were captured using uncoated silicon nitride DNP-S-10 (Veeco, Camarillo, CA) AFM cantilevers with a typical spring constant of 0.12 N/m. Contact mode topographic images were collected at scan rates of 0.7-1 Hz, and continuous adjustments to the set point kept the force exerted on the sample at a minimum. Scans were collected at 512 x 512 pixel resolution and were line fitted with first- to third-order polynomials when necessary.

Solid-supported bilayers of the desired composition were prepared, and fluorescence and AFM images of the same sample area were acquired sequentially after first assessing sample

homogeneity over several areas by fluorescence. The sample was photolyzed for the specified period of time and fluorescence or correlated images were recorded to monitor changes in the bilayer morphology. Typically fluorescence images were acquired before and after AFM scans of the same area to check for changes in membrane morphology occurring during or due to scanning.

RESULTS

Photo-uncaging of 1 in phase separated bilayers. Caged Cer **1** was incorporated in DOPC/ ESM/ Chol mixtures which form bilayers with coexisting L_d and L_o phases. These mixtures have been extensively used by several groups, including our own, to study enzymatic Cer generation in model membranes that mimic the phase separation behavior of rafts in cellular membranes.[17, 19, 21, 22, 36] Figure 1 shows a representative example of a planar supported bilayer formed in the dark from a quaternary mixture of DOPC/ESM/Chol/**1** in 8/7/4/1 molar ratios and containing 0.5 mol % DiI-C_{20} in water. The DiI-C_{20} fluorescence image (Figure 1A) reveals dark, micrometer-scale L_o domains in a bright L_d bulk phase, indicating that this lipophilic probe preferentially partitions into the disordered environment.[37] Although caged Cer analogs have low fluorescence quantum yields,[29] the emission of **1** can be used to visualize its relative distribution in the membrane (Figure 1B). The inverted fluorescence contrast for the coumarin channel with respect to the DiI-C_{20} image (bright L_o domains) suggests that the caged lipid is enriched in the ordered phase. Correlated DiI-C_{20} fluorescence and AFM imaging confirmed the assignment of L_o and L_d phases in the optical images (Figure 2A). Height measurements from the AFM scans showed that the ordered domains were 0.8-1 nm taller than the surrounding fluid phase. This height difference is consistent with reported values for ternary lipid mixtures of DOPC/ESM/Chol, as well as with those incorporating similar molar fractions of C16-Cer.[18, 25]

AFM and fluorescence were also used to detect and follow membrane restructuring when C16-Cer was photochemically generated in these supported bilayers. First, HPLC analysis (Figure S1, Supporting Information) confirmed the time-dependent disappearance of **1** in SUVs of DOPC/ESM/Chol/**1** in 8/7/4/1 molar ratios with 0.5 mol % DiI-C_{20} upon irradiation at 350 nm. Figure 2 illustrates a photolysis experiment in a supported bilayer formed from vesicles of the same quaternary lipid mixture where a small region of the bilayer was irradiated using the microscope lamp and aperture (λ 377 $\pm$ 25 nm) for a total of 10 min. During this time the sample was periodically monitored using both imaging techniques. Structural changes first became apparent by AFM (Figure 2B) as small pockets of lower height or slight indentations within the L_o domains. As more Cer was generated with an extended irradiation time, the size and frequency of these features increased, and the largest pockets were detectable by fluorescence (Figure 2C, arrows) with intensities that were similar to the fluid phase. Closer examination of the AFM scans showed that these pockets were at approximately the same height as the L_d phase. The bilayer continued to evolve immediately after photolysis (Figure 2D), but its morphology remained unchanged after approximately 20 min. This

suggests that the short-term reorganization of membrane lipids to accommodate the de novo Cer was complete.

Repeated AFM scanning of a bilayer after photochemical Cer generation appeared to accelerate the dissolution of L_o domains, particularly in sample regions where smaller sized domains predominated (Figure S2). Therefore, further uncaging experiments in which the area of interest was monitored exclusively by fluorescence were conducted in order to assess the extent of bilayer restructuring in the absence of any mechanical perturbation caused by the scanning AFM tip. Figure 3 illustrates the progressive disappearance of ordered domains in a typical sample containing 5 mol % **1**. After imaging an area of the initial bilayer (Figure 3A), we closed the aperture on the microscope illuminator to give a ~25-μm diameter illumination area for generation of C16-Cer (Figure 3B). The region of interest was irradiated for 30 min and the sample was then monitored for an additional 20 min. By this point the bilayer had attained a stable morphology with a significantly decreased surface coverage of the L_o domains and the complete disappearance of some smaller domains. Fully opening the aperture identified adjacent areas of the bilayer where no Cer had been generated, providing a clear *in situ* comparison of pre- and post-UV membrane morphology (Figure 3A, C).

A control experiment in which a DOPC/ESM/Chol 2/2/1 bilayer containing 0.5 mol % DiI-C_{20} was irradiated for a comparable period of time showed no changes in membrane morphology in the absence of caged Cer (Figure S3). Lipid mixtures containing 5 mol % C16-Cer were also prepared to form bilayers of DOPC/ESM/Chol/C16-Cer in 8/7/4/1 molar ratios and stained with 0.5 mol % DiI-C_{20}. AFM images of these samples showed L_o/L_d phase separation with domains that were of similar size, shape, and height above the fluid phase to those formed from mixtures with 5 mol % **1** or no Cer. We typically observed some variability in domain shape and size within and between individual samples for phase-separated supported bilayers that contain Cer. This variability may be attributed to local sample-substrate effects and/or subtle differences in the sample's thermal history.[38]

We then examined the effects of generating higher mole fractions of C16-Cer. Bilayers of DOPC/ESM/Chol/**1** in an 8/6/4/2 molar ratio and containing 0.5 mol % DiI-C_{20} present coexisting L_o/L_d phases with domains comparable to those observed at 5 mol % **1** (Figure 4). After 30 min of UV irradiation, similar indentations in the ordered domains were observed, with some fragmentation of large domains and disappearance of small domains. The AFM and fluorescence images of these samples were qualitatively similar to those obtained for bilayers with a lower mol fraction of **1** and provide no evidence for formation of the Cer-rich subdomains that have been observed previously upon both direct and enzymatic Cer generation in similar ternary lipid mixtures.[14, 15, 18, 22, 25] Several attempts were made to incorporate a larger fraction of **1** in order to generate more Cer in the supported bilayers. Supported bilayers prepared from DOPC/ESM/Chol vesicles with up to 20 mol % of **1** were densely covered with vesicles that could not be removed by extensive washing. After UV irradiation of these samples most of the adsorbed vesicles had disappeared; Cer generation in the vesicles may have promoted vesicle rupturing or desorption. Only modest restructuring of the underlying

bilayers took place, on a scale comparable to that observed in the samples incorporating 5 or 10 mol % Cer. This suggests that a significant fraction of **1** may be in the adsorbed vesicles, leading to lower than expected concentrations of **1** in the supported bilayer. Attempts to incorporate **1** in a preformed bilayer by incubation with a 50 μM aqueous suspension (with 0.5 % ethanol) were not successful, as judged by lack of change in the bilayer following UV irradiation.

Photo-uncaging of 2 in phase-separated bilayers. Photolysis of caged C4 Cer, **2**, in DOPC/ESM/Chol lipid bilayers gave qualitatively similar results to those obtained for **1**. A bilayer prepared from DOPC/ESM/Chol/2 (8:7:4/1 molar ratio, 0.5 mol % DiI-C_{20}) showed a similar pattern of dark L_o domains surrounded by a bright fluid phase in the DiI channel (Figure 5A). The reversal in fluorescence contrast in the coumarin channel is consistent with enrichment of **2** in the L_o domains (Figure 5B). The fluorescence contrast in the coumarin channel was slightly higher than that obtained for bilayers containing **1**. Changes in bilayer fluorescence after UV irradiation were followed by fluorescence (Figure 5B-E); parallel to the results for **1**, small regions of fluid phase appeared in the initial Lo domains. Interestingly, in this case the improved contrast in the coumarin channel allowed the changes in bilayer morphology to be followed in both fluorescence channels (Figure 5E). The difference between irradiated and unirradiated areas of the bilayer are evident when the bilayer is imaged with the microscope aperture opened, as shown in the larger scale images of the same bilayer measured before and after UV irradiation (Figure S4).

A correlated AFM-fluorescence experiment was also carried out for a DOPC/ESM/Chol/**2** bilayer, as presented in Figure 6. Fluorescence images showed morphology changes similar to those in Figure 5 and the corresponding before and after UV AFM images confirmed the appearance of many small regions of lower phase in the initial L_o domains. The height of the L_o domains was slightly lower (0.4 – 0.6 nm) than for L_o domains in bilayers containing the C16 analog, **1**, both before and after photolysis of **2**.

DISCUSSION

Incorporation of caged Cer **1** did not modify the morphology of the ternary lipid bilayers that we have used to model membrane rafts, nor did it lead to a significant change in the height difference between the ordered domains and the surrounding fluid phase. The coumarin fluorescence is slightly more intense in the ordered domains, consistent with enhanced partitioning of **1** into the ordered phase. However, fluorescence intensity ratios do not give quantitative information about the probe partition coefficient since they may be affected by differences in probe brightness and orientation of the fluorophore dipole between the two phases.[37] Photolysis of **1** leads to changes in the bilayer morphology, most notably a progressive decrease in domain size and in some cases the complete disappearance of the domains. Correlated AFM and fluorescence imaging indicate that small fluorescent regions appear in some L_o domains; both the height and fluorescence intensity of these features are

similar to those of the bulk L_d phase. Similar changes are observed when bilayers are prepared with either 5 or 10 mol % **1**. The domain reorganization is consistent with significant partitioning of the caged Cer into the ordered domains, as also suggested by the coumarin fluorescence images. Irradiations of small bilayer regions clearly demonstrate that the photo-uncaging strategy allows for temporal and spatial control over the bilayer morphology.

Several AFM studies have demonstrated that bilayers formed from vesicles in which long-chain Cer (C16 or C18) has been premixed with ternary lipid mixtures display Cer-enriched domains in addition to L_o domains and a fluid phase.[14-16, 18, 25] These studies indicate that ~8% Cer is required for the formation of detectable domains in SM/DOPC/Chol membranes. Similarly, in situ Cer generation by SMase treatment of preformed SM-containing bilayers results in the formation of new Cer-enriched regions, although the overall morphology is much more complex for enzyme-treated bilayers.[14, 17, 19, 22] By contrast to these results, photolysis of **1** provides no evidence for the formation of a new Cer-enriched phase, although there are clear changes in bilayer morphology when Cer is released in the supported bilayer. There are several possible explanations for the lack of Cer domains. Although the amount of Cer generated will be below the threshold for domain formation when 5 mol % **1** is incorporated in the initial vesicles, this is unlikely to be the case for bilayers containing 10 mol % **1**, assuming efficient photolysis of the caged compound. This assumption is supported by experiments demonstrating that photolysis of **1** and other caged Cers is rapid and efficient using several different lamps for both aqueous dispersions and vesicles solutions.[29] This is further corroborated by the observation that longer irradiation periods do not induce additional changes in bilayer morphology, consistent with photolysis of all the caged Cer.

A sub-threshold level of Cer for domain formation could also occur if the initial concentration of **1** in the supported bilayers is less than that in the initial vesicle suspension. Although it is generally assumed that the lipid ratios in supported bilayers are comparable to those in the bulk vesicle solution, several recent studies demonstrate significant heterogeneity in composition for individual vesicles within a single sample.[39-42] For example, Stamou and coworkers used a single vesicle fluorescence assay to demonstrate variations of up to an order of magnitude in the relative composition of individual liposomes.[39, 40] The heterogeneity depended on the vesicle preparation method and size, with small vesicles (e.g., SUVs) exhibiting a greater degree of heterogeneity than large vesicles (GUVs). Heterogeneity in the initial vesicle population may lead to selection of a subset of vesicles during bilayer formation via vesicle fusion, since the kinetics for vesicle adsorption and rupture are strongly affected by lipid composition as well as the surface and additives in the aqueous solution.[43] Recently we have concluded that selection for a subset of vesicles from a heterogeneous vesicle population during bilayer formation may contribute to unexpected trends in morphology for bolalipid/POPC mixtures.[44] In the present study, the presence of the bromohydroxy coumarin moiety, which is partially deprotonated at the pH used to form SUVs and supported bilayers in our experiments, may be an important factor. Variations in the net negative charge on the SUVs due to different fractions of **1** coupled with electrostatic repulsion between the vesicles

and the negatively charged surface could lead to formation of a supported bilayer with a lower mol fraction of **1** than in the bulk vesicle suspension. Consistent with this explanation, attempts to incorporate >10 mol % **1** provided no evidence for increased Cer content in the supported lipid bilayers, but did lead to many adsorbed vesicles that were difficult to remove.

Although we believe that vesicle heterogeneity and selection for a subset of vesicles with less than the bulk concentration of **1** contribute to our results, there are alternate explanations for the lack of Cer-enriched domains. Comparison of results for Cer incorporation by premixing and enzymatic generation highlight the importance of non-equilibrium effects in determining the morphology for enzyme treated bilayers.[17, 21, 25, 45] It is possible that a similar effect (i.e., non-equilibrium lipid organization) occurs when Cer is generated by photo-uncaging. Diffusion of both **1** and Cer will be considerably slower in the L_o domains (where a significant fraction of **1** resides, based on coumarin fluorescence intensities) than in a fluid DOPC bilayer. It is also possible that lipid equilibration/membrane restructuring of SMase-treated bilayers occurs more rapidly than in the absence of enzyme since insertion of hydrophobic domains and translocation of the bound enzyme may perturb lipid packing and induce local disorder. Finally, the ability of Cer to form gel-phase domains is strongly modulated by the presence of Chol; at high Chol content domains are hypothesized to be replaced by a Chol-enriched L_o phase.[13]

The incorporation of C4 caged Cer, **2**, in DOPC/SM/Chol bilayers shows a similar behavior to that obtained for the C16 analog. One important difference is the observation of a smaller height difference between the domains and fluid phase, both before and after photolysis. This is consistent with incorporation of **2** and its photolysis product in the L_o domains, in agreement with the stronger coumarin fluorescence intensity in the domains. A previous study of the effects of variable chain length Cers on bilayers with L_o domains concluded that short-chain Cers differed from long-chain C16 and C18 analogs in two respects.[15] First, they did not promote the formation of ceramide gel-phase domains. Second, they showed a strong preference for localization in L_o domains and led to a reduction in the fractional surface coverage of the domains and in the height difference between the domains and the surrounding L_d phase. Fluorescence correlation spectroscopy indicated that the diffusion coefficient for dye-labeled lipids in the L_o domains increased by a factor of 2-3 times when C6- and C2-Cers were incorporated in L_o domains, providing evidence for strong perturbation of lipid packing. By contrast, addition of C16- and C18-Cer had no effect on lipid diffusion within the domains, although they did promote the formation of Cer-enriched gel-phase domains. These results are consistent with several other studies demonstrating that short chain Cers are unable to stabilize rafts, have reduced capacity to displace Chol from ordered domains and do not readily form gel-phase domains.[46, 47] It has been suggested that perturbation of lipid packing for C4- and C6-Cer may reflect wobbling of the *N*-acyl chain between the aqueous phase and the hydrophobic core of the bilayer.[15] Finally, the addition of Cers with asymmetric chain lengths can lead to formation of mixed or partially interdigitated

phases, which would reduce the bilayer thickness.[48, 49] Overall, we conclude that the lack of Cer domains upon photolysis of **2** is consistent with the expected behavior of short-chain Cer.

Attempts to work at higher mol fraction of **1** led to samples with many adherent vesicles. Interestingly, we observed that vesicles were readily removed by photolysis, which may indicate that loss of the bromohydroxy coumarin moiety renders the individual vesicles less "sticky". It is also possible that generation of Cer promotes vesicle permeability and/or rupture. In this context, a number of recent examples have demonstrated that incorporation of photoswitchable surfactants or amphiphiles can be used to trigger membrane permeability for applications such as drug delivery.[50-52] Chemical generation of Cer by coupling of sphingosine to fatty acid salts in lipid bilayers has been shown to alter membrane properties and promote vesicle fusion.[53] Experiments aimed at testing the suitability of caged Cer photolysis for triggering vesicle permeability are underway in our laboratory.

Two recent studies have employed the photoisomerization of azobenzene to control lipid organization in bilayer membranes. In one example, cis-trans isomerization of an azobenzene moiety attached to the hydroxyl group of Chol induced shape changes in GUVs and disrupted liquid-ordered domains, leading to their disappearance or the incorporation of fluid phase regions.[54] A more recent example used photoisomerization of an azobenzene – substituted amphiphile to promote phase separation for lipid mixtures with compositions close to a phase boundary.[33] Changes in line tension due to conversion of trans-azobenzene localized in the bilayer headgroup region to the more bulky cis isomer were postulated to be the origin of the observed effects.

CONCLUSIONS

In summary, the photorelease of Cer from caged molecules provides a method to modulate lipid organization with both spatial and temporal control. The generation of C16-Cer via photo-uncaging of **1** in DOPC/SM/Chol bilayers leads to changes in L_o domains that are distinct from both the direct incorporation of Cer and enzymatic Cer generation, most notably the lack of Cer-rich gel-phase domains. The differences are believed to reflect low incorporation of **1** in supported bilayers due to a heterogeneous population of vesicles and selective adsorption and rupture of vesicles containing low concentrations of caged Cer during bilayer formation, although non-equilibrium lipid mixing may also contribute. Photorelease of a short-chain Cer results in qualitatively similar results, with disappearance of some L_o domains, but also with a smaller height difference between the ordered and disordered phases. These results are consistent with literature results demonstrating that a short-chain Cer disrupts L_o domains and does not form Cer-rich gel phases, but may form mixed or partially interdigitated phases.

ASSOCIATED CONTENT

Supporting Information

Four figures with additional AFM and fluorescence images documenting the photolysis of **1** in vesicle solution and the effects of incorporation and photoysis of **1** and **2** on supported lipid bilayers.

AUTHOR INFORMATION

Corresponding Author

Linda.Johnston@nrc-cnrc.gc.ca

Notes

The authors declare no competing financial interests.

ACKNOWLEDGMENTS

DMCR and LJJ thank the Natural Sciences and Engineering Research Council for support in the form of a postgraduate scholarship and a Discovery Grant. RB acknowledges support from NIH Grant HL-083187. SPP acknowledges support from the Reactive Intermediates Student Exchange program.

FIGURE CAPTIONS

Figure 1. Epifluorescence images of a planar supported lipid bilayer composed of DOPC/ESM/Chol/**1** (8/7/4/1 molar ratio, labeled with 0.5 mol % DiI-C_{20}). (A) L_o domains appear dark in the DiI channel indicating that DiI-C_{20} is enriched in the L_d phase; (B) inverted contrast for the coumarin fluorescence image of the same area suggests that the caged ceramide preferentially partitions into the ordered phase. Scale bar = 4 μm.

Figure 2. Caged C16-Cer photolysis in a DOPC/ESM/Chol/**1** supported bilayer (8/7/4/1 molar ratio, 0.5 mol% DiI-C_{20}). The correlated fluorescence and AFM images reveal the progressive morphological changes that occur in the L_o domains as Cer is generated. (A) $T_{0\ min}$ before UV irradiation; (B) $T_{15\ min}$ after 5 min UV irradiation; (C) $T_{30\ min}$ after a second 5 min UV irradiation; (D) $T_{50\ min}$ after an additional 20 min dark equilibration. Scale bar = 3 μm.

Figure 3. Caged C16-Cer photolysis in a DOPC/ESM/Chol supported bilayer (8/7/4/1 molar ratio, 0.5 mol % DiI-C_{20} in water). As increasing amounts of Cer are generated with longer irradiation times, L_o domains decrease in size and gradually disappear. (A) $T_{0\ min}$ before photolysis; (B) closed aperture indicating the region to be irradiated (C) $T_{50\ min}$ 20 min after a

30 min UV-irradiation with the aperture opened to reveal adjacent areas of the bilayer not exposed to UV light. Scale bar = 5 μm.

Figure 4. Photolysis of bilayers with 10 mol % caged Cer gives similar results to those obtained with 5 mol % **1**. A DOPC/ESM/Chol/**1** bilayer (8/6/4/2 molar ratio, 0.5 mol % DiI-C_{20}) has L_o domains of similar size and height to those obtained with 5 mol % **1**. Photochemical generation of Cer induces time-dependent lipid reorganization that can be observed by both fluorescence and AFM. (A) $T_{0\ min}$ before UV; (B) $T_{60\ min}$ 30 min after a 30 min UV irradiation; (C) AFM of the same area acquired immediately after the fluorescence image in (B). Scale bar = 2 μm.

Figure 5. Caged C4 Cer photolysis in a DOPC/ESM/Chol/**2** supported bilayer (8/7/4/1 molar ratio, 0.5 mol % DiI-C_{20}). (A, B) $T_{0\ min}$ before UV irradiation for DiI and coumarin channels; (C) $T_{5\ min}$ immediately after a 5 min UV irradiation, DiI channel; (D, E) T_{20min} 15 min after UV irradiation for DiI and coumarin channels; (F) T_{35min} 30 min after UV, DiI channel. Note that the intensity scale is lower for image E, due to release of the coumarin fluorophore into the aqueous solution as **2** is photolysed. Scale bar = 3 μm.

Figure 6. Caged C4 Cer photolysis in a DOPC/ESM/Chol/**2** bilayer (8/7/4/1 molar ratio, 0.5 mol % DiI-C_{20}). (A) $T_{0\ min}$ before UV irradiation; (B) $T_{10\ min}$ immediately after UV irradiation; (C) $T_{40\ min}$ 30 min after UV irradiation; (D, E) AFM images before UV irradiation and after image C. The morphological changes are evident in both fluorescence and AFM images but are clearer with the higher resolution available with AFM. Scale bar = 3 μm.

REFERENCES

1 Bollinger, C. R.; Teichgraber, V.; Gulbins, E. *Biochim. Biophys. Acta* **2005**, *1746*, 284-294.

2 Cremesti, A. E.; Goni, F. M.; Kolesnick, R. *FEBS Lett.* **2002**, *531*, 47-53.

3 Hannun, Y. A. *Science* **1996**, *274*, 1855-1859.

4 Hannun, Y. A.; Obeid, L. M. *J. Biol. Chem.* **2011**, *286*, 27855-27862.

5 Fanani, M. L.; Hartel, S.; Maggio, B.; De Tullio, L.; Jara, J.; Olmos, F.; Oliveira, R. G. *Biochim. Biophys. Acta* **2010**, *1798*, 1309-1323.

6 Goni, F. M.; Alonso, A. *Chem. Phys. Lipids* **2009**, *160*, S2-S2.

7 Lopez-Montero, I.; Monroy, F.; Velez, M.; Devaux, P. F. *Biochim. Biophys. Acta* **2010**, *1798*, 1348-1356.

8 Zou, S.; Johnston, L. J. *Curr. Opin. Coll. Inter. Sci.* **2010**, *15*, 489-498.

9 Simons, K.; Gerl, M. J. *Nat. Rev. Mol. Cell Biol.* **2010**, *11*, 688-699.

10 Simons, K.; Ikonen, E. *Nature* **1997**, *387*, 569-572.

11 Pike, L. J. *J. Lipid Res.* **2009**, *50*, S323-S328.

12 Edidin, M. *Annu. Rev. Biophys. Biomol. Struct.* **2003**, *32*, 257-283.

13 Castro, B. M.; Silva, L. C.; Fedorov, A.; de Almeida, R. F. M.; Prieto, M. *J. Biol. Chem.* **2009**, *284*, 22978-22987.

14 Chiantia, S.; Kahya, N.; Ries, J.; Schwille, P. *Biophys. J.* **2006**, *90*, 4500-4508.

15 Chiantia, S.; Kahya, N.; Schwille, P. *Langmuir* **2007**, *23*, 7659-7665.

16 Sullan, R. M. A.; Li, J. K.; Zou, S. *Langmuir* **2009**, *25*, 12874-12877.

17 Carrer, D. C.; Kummer, E.; Chwastek, G.; Chiantia, S.; Schwille, P. *Soft Matter* **2009**, *5*, 3279-3286.

18 Carter Ramirez, D. M.; Ogilvie, W. W.; Johnston, L. J. *Biochim. Biophys. Acta* **2010**, *1798*, 558-568.

19 Chao, L.; Gast, A. P.; Hatton, T. A.; Jensen, K. F. *Langmuir* **2010**, *26*, 344-356.

20 Lopez-Montero, I.; Velez, M.; Devaux, P. F. *Biochim. Biophys. Acta* **2007**, *1768*, 553-561.

21 Ira; Johnston, L. J. *Biochim. Biophys. Acta* **2008**, *1778*, 185-197.

22 Ira; Zou, S.; Carter Ramirez, D. M.; Vanderlip, S.; Ogilvie, W.; Jakubek, Z.; Johnston, L. J. *J. Struct. Biol.* **2009**, *168*, 78-79.

23 Silva, L. C.; de Almeida, R. F. M.; Castro, B. M.; Prieto, M. *Biophys. J.* **2007**, 355A-355A.

24 Sot, J.; Ibarguren, M.; Busto, J. V.; Montes, L. R.; Goni, F. M.; Alonso, A. *FEBS Lett.* **2008**, *582*, 3230-3236.

25 Ira; Johnston, L. J. *Langmuir* **2006**, *22*, 11284-11289.

26 Brieke, C.; Rohrbach, F.; Gottschalk, A.; Mayer, G.; Heckel, A. *Angew. Chem., Int. Ed. Engl.* **2012**, *51*, 8446-8476.

27 Lee, H.-M.; Larson, D. R.; Lawrence, D. S. *ACS Chem. Biol.* **2009**, *4*, 409-427.

28 Yu, H.; Li, J.; Wu, D.; Qiu, Z.; Zhang, Y. *Chem. Soc. Rev.* **2010**, *39*, 464-473.

29 Kim, Y. A.; Carter Ramirez, D. M.; Costain, W. J.; Johnston, L. J.; Bittman, R. *Chem. Commun.* **2011**, *47*, 9236-9238.

30 Lankalapalli, R. S.; Ouro, A.; Arana, L.; Gomez-Munoz, A.; Bittman, R. *J. Org Chem.* **2009**, *74*, 8844-8847.

31 Mentel, M.; Laketa, V.; Subramanian, D.; Gillandt, H.; Schultz, C. *Angew. Chem., Int. Ed.* **2011**, *50*, 3811-3814.

32 Shigenaga, A.; Hirakawa, H.; Yamamoto, J.; Ogura, K.; Denda, M.; Yamaguchi, K.; Tsuji, D.; Itoh, K.; Otaka, A. *Tetrahedron* **2011**, *67*, 3984-3990.

33 Hamada, T.; Sugimoto, R.; Nagasaki, T.; Takagi, M. *Soft Matter* **2011**, *7*, 220-224.

34 Hamada, T.; Sugimoto, R.; Vestergaard, M. C.; Nagasaki, T.; Takagi, M. *J. Am. Chem. Soc.* **2010**, *132*, 10528-10532.

35 Liu, X.-M.; Yang, B.; Wang, Y.-L.; Wang, J.-Y. *Biochim. Biophys. Acta* **2005**, *1720*, 28-34.

36 Silva, L. C.; Futerman, A. H.; Prieto, M. *Biophys. J.* **2009**, *96*, 3210-3222.

37 Baumgart, T.; Hunt, G.; Farkas, E. R.; Webb, W. W.; Feigenson, G. W. *Biochim. Biophys. Acta* **2007**, *1768*, 2182-2194.

38 Blanchette, C. D.; Lin, W.-C.; Ratto, T. V.; Longo, M. L. *Biophys. J.* **2006**, *90*, 4466-4478.

39 Elizondo, E.; Larsen, J.; Hatzakis, N. S.; Cabrera, I.; Bjornholm, T.; Veciana, J.; Stamou, D.; Ventosa, N. *J. Am. Chem. Soc.* **2012**, *134*, 1918-1921.

40 Larsen, J.; Hatzakis, N. S.; Stamou, D. *J. Am. Chem. Soc.* **2011**, *133*, 10685-10687.

41 Buboltz, J. T.; Bwalya, C.; Williams, K.; Schutzer, M. *Langmuir* **2007**, *23*, 11968-11971.

42 Veatch, S. L.; Keller, S. L. *Biochim. Biophys. Acta* **2005**, *1746*, 172-185.

43 Richter, R. P.; Berat, R.; Brisson, A. R. *Langmuir* **2006**, *22*, 3497-3505.

44 Mulligan, K.; Brownholland, D.; Carnini, A.; Thompson, D. H.; Johnston, L. J. *Langmuir* **2010**, *26*, 8525-8533.

45 Fanani, M. L.; De Tullio, L.; Hartel, S.; Jara, J.; Maggio, B. *Biophys. J.* **2009**, *96*, 67-76.

46 Megha; Sawatzki, P.; Kolter, T.; Bittman, R.; London, E. *Biochim. Biophys. Acta* **2007**, *1768*, 2205-2212.

47 Nyholm, T. K. M.; Grandell, P.-M.; Westerlund, B.; Slotte, J. P. *Biochim. Biophys. Acta* **2010**, *1798*, 1008-1013.

48 Carrer, D. C.; Schreier, S.; Patrito, M.; Maggio, B. *Biophys. J.* **2006**, *90*, 2394-2403.

49 Pinto, S. N.; Silva, L. C.; de Almeida, R. F. M.; Prieto, M. *Biophys. J.* **2008**, *95*, 2867-2879.

50 Diguet, A.; Yanagisawa, M.; Liu, Y.-J.; Brun, E.; Abadie, S.; Rudiuk, S.; Baigl, D. *J. Am. Chem. Soc.* **2012**, *134*, 4898-4904.

51 Sebai, S. C.; Milioni, D.; Walrant, A.; Alves, I. D.; Sagan, S.; Huin, C.; Auvray, L.; Massotte, D.; Cribier, S.; Tribet, C. *Angew. Chem., Int. Ed. Engl.* **2012**, *51*, 2132-2136.

52 Uda, R. M.; Hiraishi, E.; Ohnishi, R.; Nakahara, Y.; Kimura, K. *Langmuir* **2010**, *26*, 5444-5450.

53 Kunishima, M.; Tokaji, M.; Matsuoka, K.; Nishida, J.; Kanamori, M.; Hoki, K.; Tani, S. *J. Am. Chem. Soc.* **2006**, *128*, 14452-14453.

54 Yasuhara, K.; Sasaki, Y.; Kikuchi, J. *Colloid. Polym. Sci.* **2008**, *286*, 1675-1680.

Figure 1. Epifluorescence images of a planar supported lipid bilayer composed of DOPC/ESM/Chol/**1** (8/7/4/1 molar ratio labeled with 0.5 mol % DiI-C_{20}). (A) L_o domains appear dark in the DiI channel indicating that DiI-C_{20} is enriched in the L_d phase; (B) inverted contrast for the coumarin fluorescence image of the same area suggests that the caged ceramide preferentially partitions into the ordered phase. Scale bar = 4 μm.

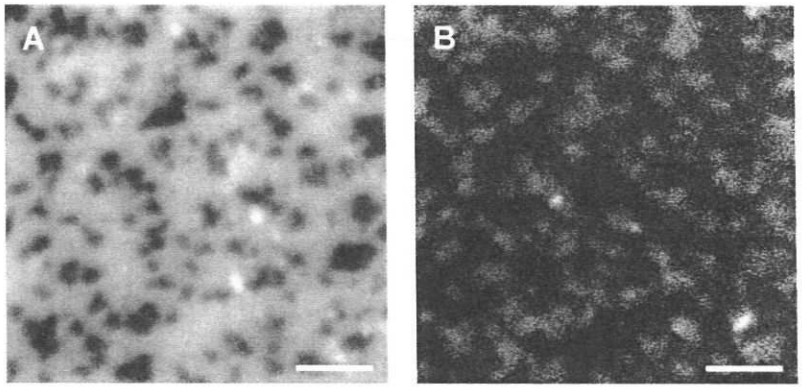

Figure 2. Caged C16 Cer photolysis in a DOPC/ESM/Chol/**1** supported bilayer (8/7/4/1 molar ratio, 0.5 mol% DiI-C_{20}). The correlated fluorescence and AFM images reveal the progressive morphological changes that occur in the L_o domains as Cer is generated. (A) $T_{0\ min}$ before UV irradiation; (B) $T_{15\ min}$ after 5 min UV irradiation; (C) $T_{30\ min}$ after a second 5 min UV irradiation; (D) $T_{50\ min}$ after an additional 20 min dark equilibration. Scale bar = 3 μm.

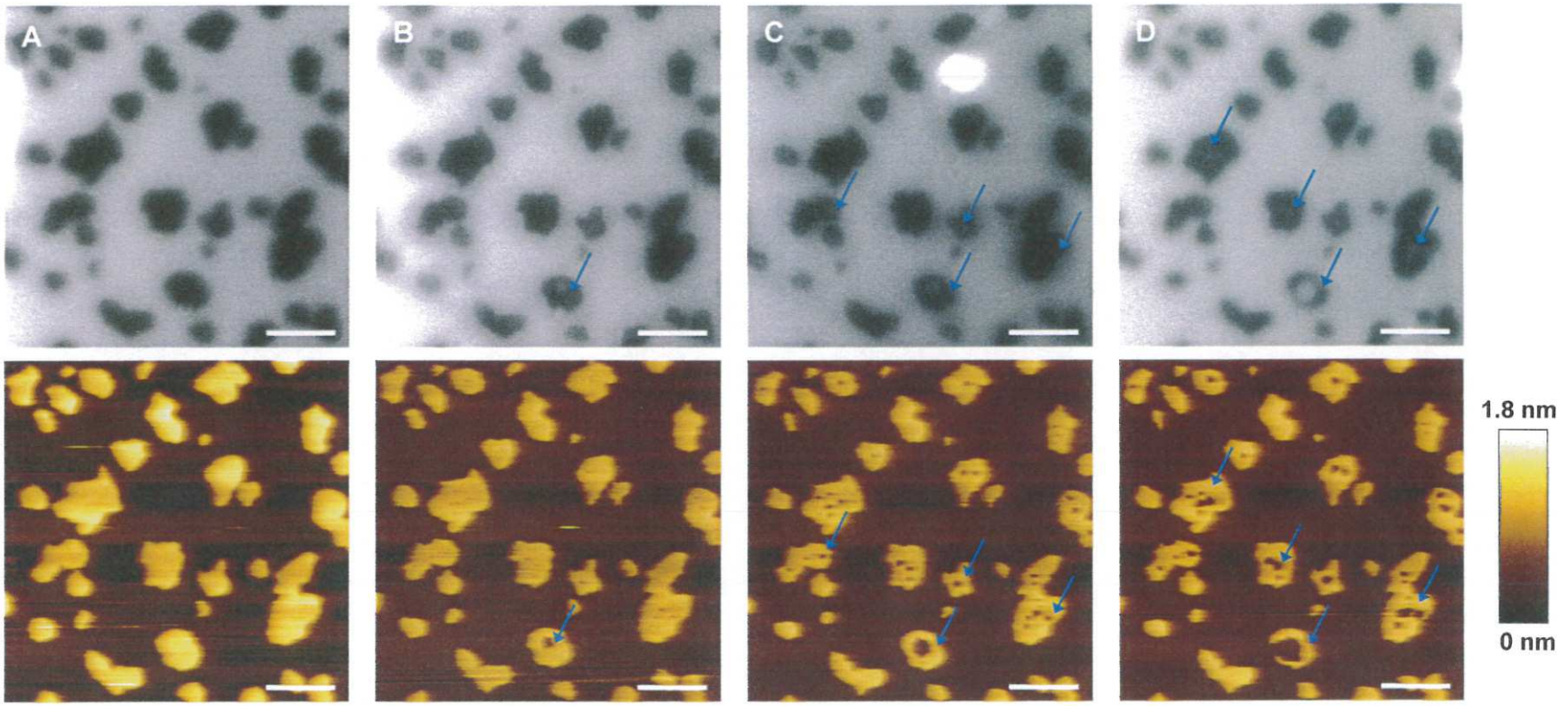

Figure 3. As increasing amounts of Cer are generated with longer irradiation times, L_o domains in a DOPC/ESM/Chol/**1** bilayer (8/7/4/1 molar ratio, 0.5 mol % DiI-C_{20} in water) decrease in size and gradually disappear. (A) $T_{0\ min}$ before photolysis; (B) closed aperture indicating the region to be irradiated (C) $T_{50\ min}$ 20 min after a 30 min UV-irradiation with the aperture opened to reveal adjacent areas of the bilayer not exposed to UV light. Scale bar = 5 μm.

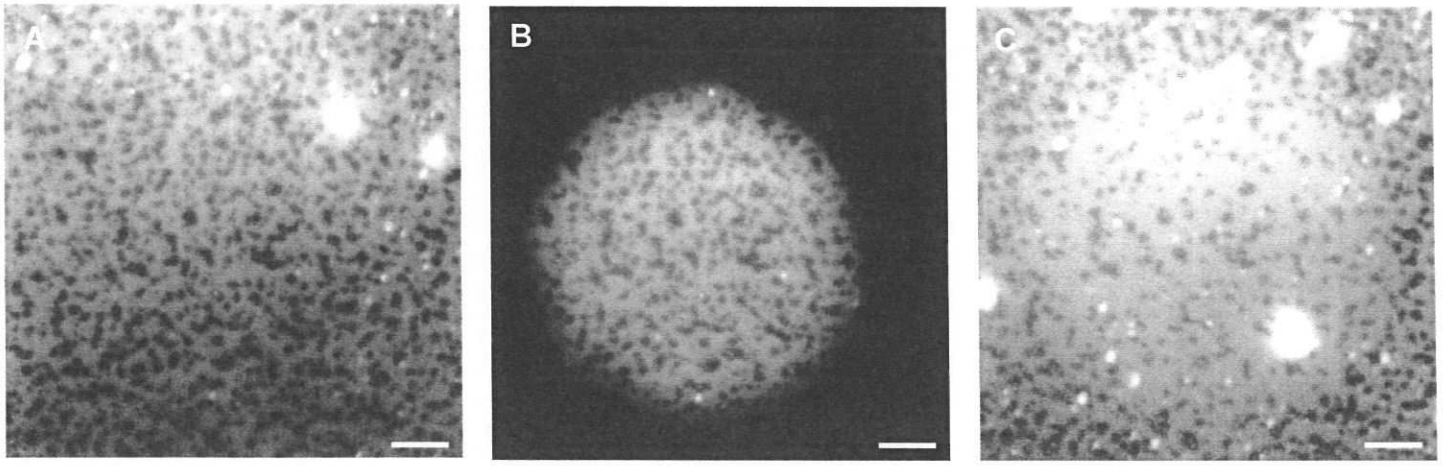

Figure 4. Increasing the caged Cer content from 5 to 10 mol % gives similar results. A DOPC/ESM/Chol/**1** bilayer (8/6/4/2 molar ratio, 0.5 mol % DiI-C_{20}) exhibits L_o domains of similar size and height to those obtained with 5 mol % **1**. Photochemical generation of Cer induces time-dependent lipid reorganization that can be observed by both fluorescence and AFM. (A) $T_{0\ min}$ before UV; (B) $T_{60\ min}$ 30 min after a 30 min UV irradiation; (C) AFM of the same area acquired immediately after the fluorescence image in (B). Scale bar = 2 μm.

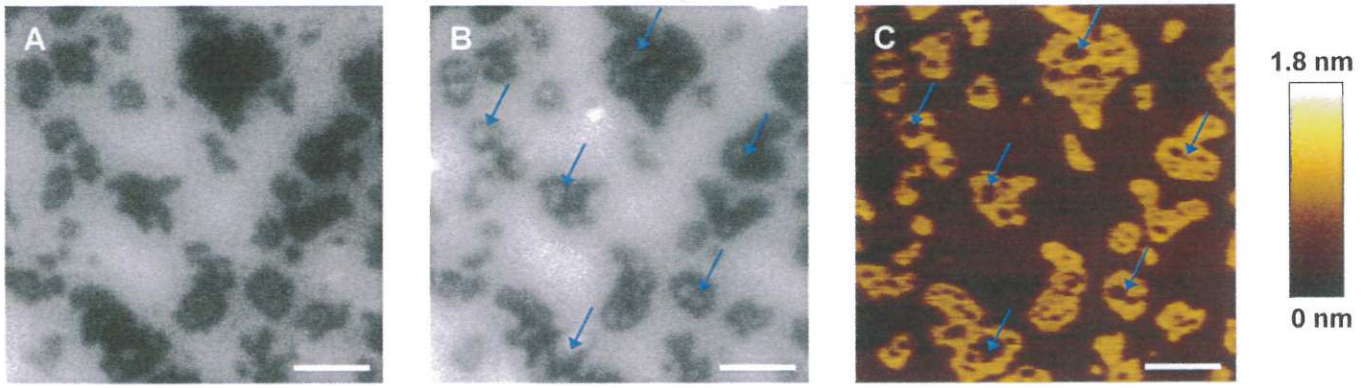

Figure 5. Caged C4 Cer photolysis in a DOPC/ESM/Chol/**2** supported bilayer (8/7/4/1 molar ratio, 0.5 mol % DiI-C_{20}). (A, B) $T_{0\ min}$ before UV irradiation for DiI and coumarin channels; (C) $T_{5\ min}$ immediately after a 5 min UV irradiation, DiI channel; (D, E) T_{20min} 15 min after UV irradiation for DiI and coumarin channels; (F) T_{35min} 30 min after UV, DiI channel. Note that the intensity scale is decreased for image E, due to release of the coumarin fluorophore into the aqueous solution as **2** is photolysed. Scale bar = 3 μm.

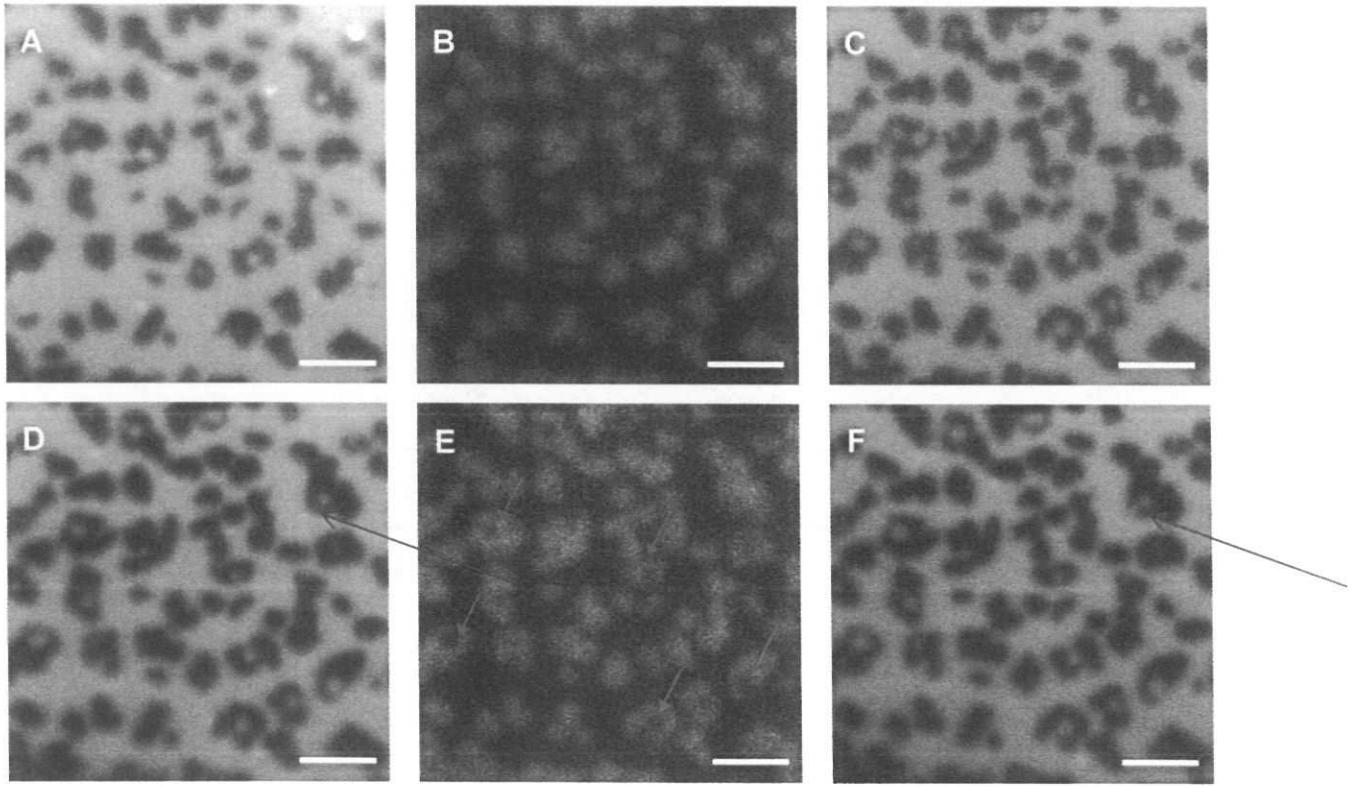

Figure 6. Caged C4 Cer photolysis in a DOPC/ESM/Chol/**2** bilayer (8/7/4/1 molar ratio, 0.5 mol % DiI-C_{20}). (A) $T_{0\ min}$ before UV irradiation; (B) $T_{10\ min}$ immediately after UV irradiation; (C) $T_{40\ min}$ 30 min after UV irradiation; (D, E) AFM images before UV irradiation and after image C. The morphological changes are evident in both fluorescence and AFM images but are clearer with the higher resolution available with AFM. Scale bar = 3 μm.